POLITECNICO DI TORINO
Repository ISTITUZIONALE

The collapse of Torrione Sucai (Mt. Viso, Italy): rockfall analysis and data calibration

Original
The collapse of Torrione Sucai (Mt. Viso, Italy): rockfall analysis and data calibration / Torsello, G., Castelli, M., Morelli, M.. - ELETTRONICO. - (2023), pp. 1162-1167. (ISRM 15th International Congress on Rock Mechanics and Rock Engineering & 72nd Geomechanics Colloquium Salzburg (Austria) October 9-14, 2023).

Availability:
This version is available at: 11583/2983366 since: 2023-10-26T10:38:13Z

Publisher:
Austrian Society for Geomechanics

Published
DOI:

Terms of use:

This article is made available under terms and conditions as specified in the corresponding bibliographic description in the repository

Publisher copyright

(Article begins on next page)

11 November 2026

The collapse of Torrione Sucai (Mt. Viso, Italy): rockfall analysis and data calibration

Giulia Torsello
Politecnico di Torino, Dipartimento di Ingegneria Strutturale, Edile e Geotecnica, Torino, Italy

Marta Castelli
Politecnico di Torino, Dipartimento di Ingegneria Strutturale, Edile e Geotecnica, Torino, Italy

Michele Morelli
ARPA Piemonte – Agenzia Regionale per la Protezione Ambientale, Torino, Italy

ABSTRACT: In December 2019 a large collapse affected the Torrione Sucai, a rocky structure located on the North-Eastern slope of Mt. Viso (Italy) at about 3100 m a.s.l. Mt Viso has been included in the UNESCO World Heritage Sites since 2013 as a biosphere reserve. Therefore, hazard and risk assessment is a priority for the protection of people and the environment. The rockfall was triggered by a combination of high fracturing of the rock mass and permafrost degradation, with associated phenomena that weakened the rock mass and created conditions for slope instability. This study entails a multi-scale analysis of fracture distribution and intersections, in order to identify the zones most prone to collapse. Moreover, a multi-scale back analysis of the run-out behavior of the 2019 rockfall was performed. The results were used to calibrate preliminary susceptibility analyses for the entire area, presented and discussed in the paper.

Keywords: climate change, permafrost degradation, rockfall, Italian Alps, Mt. Viso.

1 INTRODUCTION

Mt. Viso, located in North-Western Italy, is one of the highest peaks in the Alps (3841 m a.s.l.). The rise in temperature at the ground surface in the periglacial mountain environment results in an increase in the extension of the active layer, i.e., the zone where the temperature fluctuates around zero. The freeze and thaw cycles occurring in the active layer induce damage to the rock mass and can lead to progressive failures affecting the stability of rock slopes (James et al. 2019). This phenomenon is occurring with increasing frequency in the Mt. Viso area, as witnessed by the significant accumulation of large blocks observed at the foot of the slope. The last noteworthy episode of instability dates back to December 2019, when a large collapse occurred at 3100 m a.s.l. Hazard and risk analyses for rock instability problems should thus be extended to the entire areas affected by permafrost degradation, to highlight the most critical zones, where more in-depth geo-structural and geo-mechanical studies can be performed.

In this paper, in-depth geological-structural studies, geo-statistical elaborations, and multi-scale run-out analyses were performed to extend the landslide hazard analysis to the entire North-Eastern slope of Mt. Viso. These studies allowed to preliminary estimate: i) the potential rockfall sources, ii)

the potential unstable rock block size, and iii) their run-out areas in case of instability; iv) the most critical zones, where actions can be taken to mitigate the impact on people and environment.

2 DECEMBER 2019 ROCKFALL EVENT

The rockfall was triggered at the summit of the Torrione Sucai, at about 3100 m a.s.l. (Figure 1), where rock volume is estimated at 60000 and 80000 m^3. The propensity of this sector of the slope to generate rockfalls was already evidenced by the pre-existing accumulation of collapsed material at the base of the slope. The detachment involved a rock mass sector extended about 150-160 m vertically, about 40 m horizontally at its summit, and about 70 m near its base. It is not possible at present to establish the thickness of the mobilized mass but it can reasonably be assumed that it does not exceed 10 m. The rockfall accumulation covered an area of about 65000 m^2 with a mean thickness of about 1 m. The block size distribution over the accumulation zone is classified according to the kinetic energy, with larger blocks up to 500 m^3, distributed on the lower edge, at an elevation of about 2500 m a.s.l. (ARPA Piemonte 2021).

Permafrost distribution analysis and superficial and in-depth monitoring of temperature variation with time (Paro & Guglielmin 2014), allowed ARPA Piemonte to hypothesize that the rockfall was caused by the state of stress induced in the rock mass by permafrost degradation, with the geo-structural condition of the slope being a predisposing cause to instability.

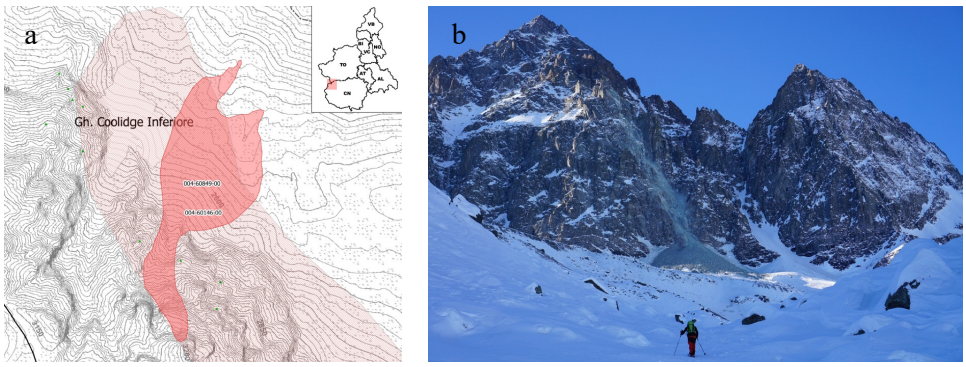


Figure 1. 2019 rockfall event. a: invasion area; b: in-situ situation after the event (ARPA Piemonte 2021).

3 GEO-STRUCTURAL ANALYSES

The photo interpretation of a post-event 3D scene processed from ortho-rectified aerial images and detailed altimetric models produced from Unmanned Aerial Vehicle (UAV) surveys were used for the geo-structural analysis (Figures 2 and 3). The images have a maximum ground resolution of 3 cm, while the 3D digital altimetric model of the surfaces has a resolution of 6 cm. A 3D dense point cloud was generated from the same images (ARPA Piemonte 2021).

Two criteria were applied for discontinuity systems identification, at different observation scales (Fell et al. 2008). First, at the site-specific, detailed scale (<1:5000), an automatic detection by means of the GPL CloudCompare software and the Facets plugin for 3D point cloud processing and analysis (CloudCompare 2021) was carried out. Due to the large area and the wide scattering of data, this analysis was performed on eight minor sectors around the detachment area. Four main geometrical discontinuity-facets systems were recognized (Figure 2), with heterogeneous distribution around the detachment area: i) a conjugate system (S1-S1a) with N-S mean dip direction and about 85° dip, widespread along the SW boundary of the detachment zone; ii) a conjugate system (S2) with E-W mean dip direction and 60-70° dip, mainly observed in the E and W sectors; iii) a system (S3) with NNE dip direction and 40-50° dip, evident in the SW sector and around the detachment area; iv) a system (S4) with NW mean dip direction and 50-60° dip, mainly distributed around the NW lateral side of the detachment area.

At the local and large scale (1:5000 - 1:25000), the recognition and classification of discontinuity systems were carried out in geometric-hierarchical terms on a wider area covering the whole slope. This was achieved by a visual interpretation of the rock slope on the 3D high-resolution images derived from the UAV survey (Morelli & Piana 2006). Three main structural associations (faults, shear zones, and fracture systems) were identified (Figure 3). A main conjugate fault system (F1-ZF) with E-W dip direction and sub-vertical dip (70°) can be associated to decametric shear zone, sigmoidal lithons and many hierarchic orders of subsidiary minor fault planes (F1r), with N-S average dip direction and moderate dipping (50°), and high fractured zone (Zfr). This fault system generates a high and complex fracturing condition in the rock mass, expressed through slip surfaces and stress-release fractures, and mostly drives the morphology of the main drainage pattern of Mt. Viso massif. A second fault system (F2), with NNE dip direction and high dip (70°), mainly consists of sub-parallel fault segments that sometimes delimit lithons with sigmoidal to wedge-shaped geometry. This system is principally characterized by multi-decametric to hectometric linear and curvilinear segments and is well represented in the NW sector of the studied area. Again, the geometric relationship between this fault system and the slope orientation makes it coherent with the development of sliding instability mechanisms. Moreover, all the morphological surfaces oriented transversely to the mean axial direction of the Mt. Viso massif are set on this system. A third fracture system (K1), with NNW dip direction and average high angle dip, consists of sub-parallel minor fractures that usually display a more regular setting. It is homogeneously spread over the whole Mt. Viso area.

The integration of the two approaches allowed the identification of the structural and geometrical patterns of faults at multiple scales, which were characterized by a rather high degree of tectonic deformation and high fracture density. According to the high-quality images of the detachment area following the 2019 event, a sliding mechanism in the NW direction may be assumed, involving the F2 and the F1r fault systems, with tension cracks and lateral release due to the high fracture density.

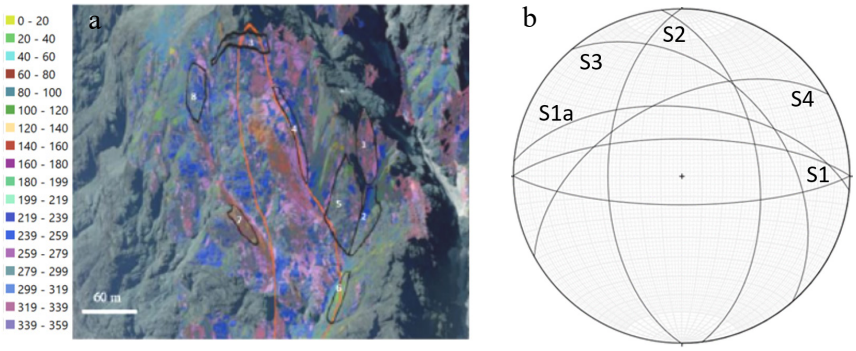


Figure 2. a: discontinuity-facets draped on AGEA 2012 orthophoto clustered in 20 classes of orientation; b: equal-area stereoplot (lower hemisphere) with the orientation of the representative planes of the main system.

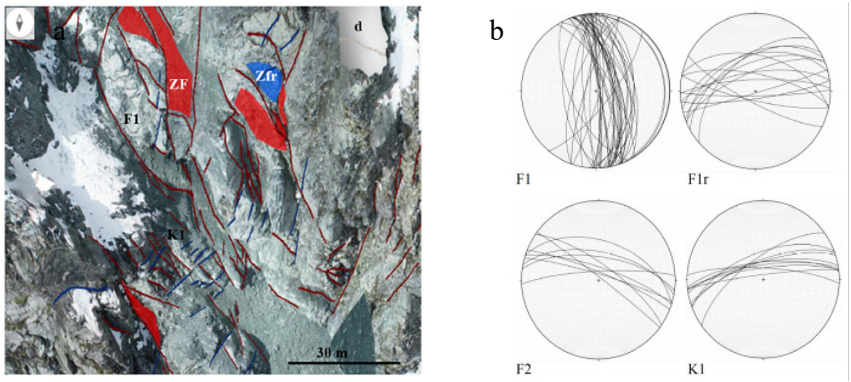


Figure 3. a: geo-structural associations by 3D digital altimetric model (detachment area). Red lines: F1-ZF fault system, blue lines: K1 fracture system, red areas: ZF fault zones, blue area: Zfr high fracture density zones; b: equal-area stereoplots (lower hemisphere) with fault orientation (F1, F2, F1r) and fractures (K1).

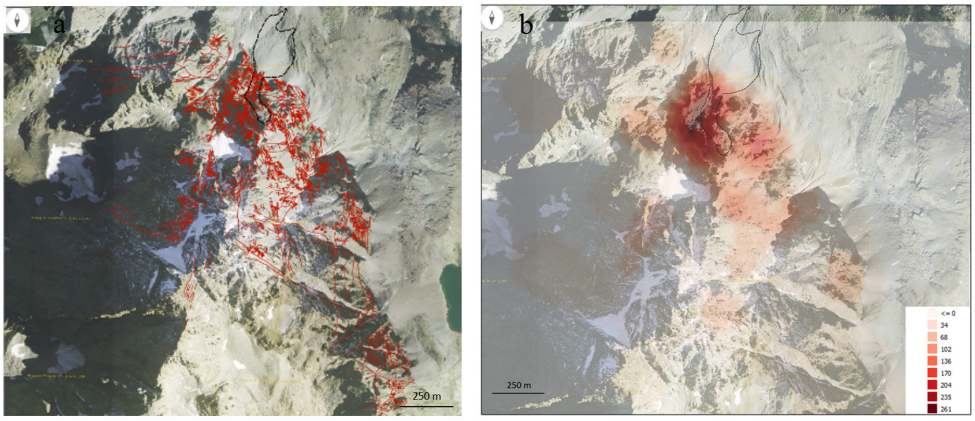


Figure 4. a: map of discontinuity systems identified on the NE slope of Mt Viso massif; b: map of discontinuity intersection density obtained by geo-statistical analysis (the legend shows the density classes).

Figure 4 shows the map of hierarchic discontinuity elements identified at the large scale (Figure 4a) and the map of fracture intersection density (Figure 4b). They highlight areas most prone to generate rockfall. These elaborations will be the basis for a preliminary rockfall hazard study of the whole area (large scale), as shown in the following sections.

4 BACK ANALYSIS OF THE ROCKFALL EVENT (DECEMBER 2019)

Two methodologies were applied in the back analysis of the December 2019 rockfall event. First, rockfall trajectories were simulated by means of a detailed, 3D, hybrid approach. Rockyfor3D software was used (Dorren 2015) to gain information about the falling blocks as well as the slope and the run-out area features. A multi-scale analysis of surface roughness was made in the accumulation zone to acquire data regarding the distribution of obstacles to rockfall. Hence, different resolutions of DEM were analyzed through terrain-analysis tools available in QGIS, and the obtained statistical distribution of asperities was used to calibrate the input parameters for the analysis. In the second methodology, the QPROTO plugin for QGIS (Castelli et al. 2021) allowed to qualitatively understand the correlation between the volume of the falling block and the run-out of the rockfall phenomenon. The plugin relies on a simplified energy approach in which the falling block path is represented by an equivalent sliding motion along a straight line (energy line) connecting the location of the farthest observed fallen block to the rockfall source point (Jaboyedoff & Labiouse 2011). The inclination of the energy line with respect to the horizontal (energy angle φ_p) represents a global block-slope friction angle, taking into account all the dissipative phenomena occurring throughout the rockfall run-out. A viewshed analysis (*r.viewshed* module of GRASS 7) is performed, starting from a pre-determined set of viewpoints assumed as rockfall source points. From each of these points, a visibility cone is defined through the angles ω (dip direction of the slope in the point), φ_p (energy angle), and α (lateral spreading angle). The intersection between the visibility cone and the surface of the slope defines the limits of the rockfall run-out area.

The same rockfall source zones were considered in both approaches, extracted by an accurate photo interpretation and a qualitative comparison between contour lines. A statistical analysis of the potentially unstable blocks acquired from the geo-structural investigation (Figure 5b) and the observation of high-quality images of the accumulated debris were used to estimate block volume. Three volume scenarios were investigated with cubic blocks of 1, 10, and 100 m^3, roughly corresponding to the 60°, 75°, and 95° percentile of the cumulated volume distribution of the potentially unstable blocks.

Following the observation of block size distribution on the accumulation after the event of December 2019 a reference energy angle φ_p was assigned to each volume scenario: φ_p = 54°, 50°, and 45° for V=1, 10 and 100 m^3 respectively. The lateral spreading angle was assumed constant and equal to 22° to take into account the wide block distribution spreading in the talus slope.

5 CALIBRATION OF PRELIMINARY HAZARD ANALYSES

A quick QPROTO analysis was carried out on a larger scale to preliminary assess the susceptibility of the entire area surrounding the Torrione Sucai summit. The distribution of rock blocks produced by the intersection of hierarchic structural elements was analyzed to identify potential rockfall instabilities based on the findings of the geo-structural studies (Figure 5). Each block is characterized by the area of the bounding polygon, which can range from a few cm^3 to more than 6000 m^3. A volume was selected to calibrate the QPROTO analyses with the assumption that the thickness was 1 m. To accurately estimate the volume of potentially unstable blocks, additional in-depth geo-structural analyses and slope stability modeling are required. The results of this preliminary analysis will be used in comparative terms in this paper, deferring the examination of this aspect of the problem to future developments of the work.

The centroid of each block was later defined, and the resulting set of points was adopted as rockfall sources in the prediction scenario. The attributes required for the QPROTO analysis were associated with each point. The estimated volume and a rock density of 2600 kg/m^3 were used to compute the block mass. The parameters of the visibility cone were estimated according to the results of the back analysis of the Torrione Sucai collapse, which was assumed to be indicative of the whole area: $\alpha = 22°$, ω = aspect, and φ_p = function of block volume. Block volumes were classified in three classes, corresponding to the three scenarios (V = 1, 10 and 100 m^3). A propensity index I_D* proportional to block volume was finally assigned to each point after a normalization with respect to the maximum volume (6284 m^3).

A first analysis was performed assuming a uniform propensity index $I_D = 1$ across the whole slope. Figure 6a shows the result in terms of frequency (susceptibility) and highlights a specific zone that can be threatened by multiple sources, which indicates a high susceptibility level. A second analysis was carried out with the propensity index I_D*, characteristics of each point. Figure 6b represents the result in terms of weighted frequency (susceptibility), and the areas most affected by large block instabilities having the highest susceptibility levels.

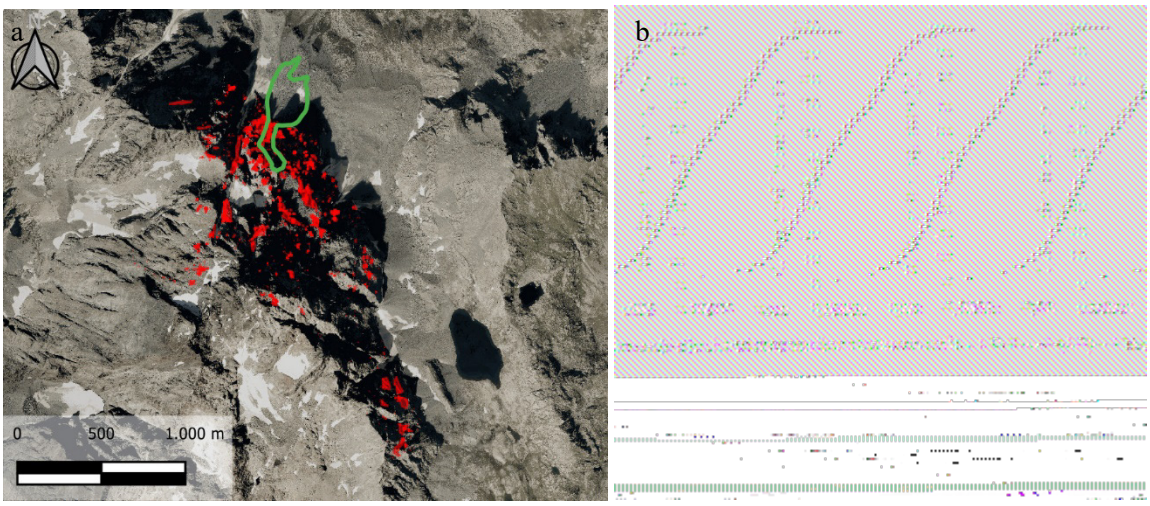


Figure 5. a: in red block distribution on the area, in green invasion area of the 2019 rockfall event (Orthophoto Regione Piemonte 2018); b: cumulated density function of estimated volumes.

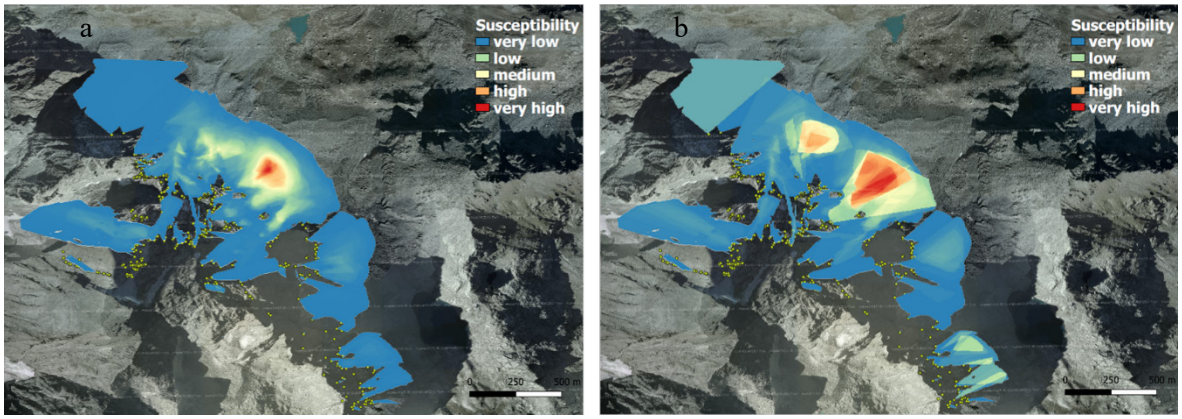


Figure 6. Results of the QPROTO analyses. a: susceptibility as rockfall frequency ($I_D = 1$); b: susceptibility as rockfall weighted frequency (I_D* function of estimated block volume).

6 CONCLUSIONS AND FURTHER DEVELOPMENTS

A preliminary susceptibility analysis was performed using the QPROTO plugin and applied to the slopes surrounding the Torrione Sucai, where a large rockfall occurred in December 2019. The results show the capability of the method to highlight the most critical zones prone to rockfall and suggest that this methodology can be useful for the preliminary assessment of rockfall risk. Future research should focus on: i) slope stability investigation to gain detailed information on potentially unstable volumes, including an assessment of permafrost distribution and climate change indicators; ii) in-depth analysis of fracture density distribution and intersections to more accurately define the location of rockfall source points iii) the examination of block size distribution on the slope and the accumulation area for a better correlation between block volume and relevant energy angles.

REFERENCES

James, S. R., Knox, h., Abbott, R., Panning, M., Screaton, E. (2019). Insights into permafrost and seasonal active-layer dynamics from ambient seismic noise monitoring. Journal of Geophysical Research: Earth Surface, 124, 1798– 1816.

ARPA Piemonte (2021). Frana del Torrione Sucai, parete NE del Mt. Viso: Scheda III livello (in Italian), from http://webgis.arpa.piemonte.it/Web22/sifrap/iii_livelli/Monviso-Sucai.pdf (accessed on 24/02/2023).

Paro, L., Guglielmin, M. (2014). Preliminary results of the research on permafrost and periglacial environment in: Piedmont Alps and future perspectives. Int. Symp. 'The Future of the Glaciers: from the past to the next 100 years', Turin (Italy) 18th - 21st September 2014.

Fell, R., Corominas, J., Bonnard, C., Cascini, L., Leroi, E., Savage,W.Z. (2008). Guidelines for landslide susceptibility, hazard and risk zoning for land-use planning. Eng. Geol. 2008, 102, 99–111.

CloudCompare [GPL software] (2021), from http://www.cloudcompare.org (accessed on 24/02/2023).

Morelli, M., Piana, F., (2006). Comparison between remote sensed lineaments and geological structures in intensively cultivated hills (Monferrato and Langhe domains, NW Italy). International Journal of Remote Sensing 27(20), 4471–4493.

Dorren, L.K.A. (2015). Rockyfor3D (v 5.2) Revealed. Transparent Description of the Complete 3D Rockfall Model. EcorisQ: Geneva (CH), 2015, from http://www.ecorisq.org/ (accessed on 24/02/2023).

Castelli, M., Torsello, G., Vallero, G. (2021). Preliminary Modeling of Rockfall Runout: Definition of the Input Parameters for the QGIS Plugin QPROTO. Geosciences 2021, 11, 88.

QPROTO plugin from https://plugins.qgis.org/plugins/qproto/ (accessed on 24/02/2023).

Jaboyedoff, M., Labiouse, V. (2011). Technical note: Preliminary estimation of rockfall runout zones. Nat. Hazards Earth Syst. Sci. 2011, 11, 819–828.